JOURNAL OF SOLID STATE CHEMISTRY 111, 257–266 (1994)

Two New Noncentrosymmetric Rubidium Titanium Phosphate Phases: $Rb_2Ti_3O_2(PO_4)_2(HPO_4)_2$ and $Rb_3Ti_3O(P_2O_7)(PO_4)_3$

William T. A. Harrison,*,[1] Thurman E. Gier,† Joseph C. Calabrese,‡ and Galen D. Stucky†

*Department of Chemistry, University of Houston, Houston, Texas 77204-5641; †Department of Chemistry, University of California, Santa Barbara, California 93106-9510; and ‡Experimental Station, E. I. Du Pont de Nemours and Company, Wilmington, Delaware 19880-0228

Received June 28, 1993; in revised form September 23, 1993, accepted September 24, 1993

Two new, noncentrosymmetric, rubidium titanium phosphate phases have been synthesized by hydrothermal and flux methods and structurally characterized by single crystal X-ray diffraction methods. $Rb_2Ti_3O_2(PO_4)_2(HPO_4)_2$ (Rb2Ti3P4) consists of a three-dimensional framework of vertex-sharing TiO_6, PO_4, and HPO_4 polyhedra interconnected via Ti–O–Ti and Ti–O–P bonds, surrounding large, one-dimensional channels occupied by eight-coordinate "guest" Rb^+ cations: these channels propagate along the a-crystallographic direction. The framework includes $[Ti_3O_{16}]$ units built up from three adjacent TiO_6 octahedra sharing *trans*-O–Ti–O links, crosslinked by the (hydrogen)phosphate groups. $Rb_3Ti_3O(P_2O_7)(PO_4)_3$ (Rb3Ti3P5) is built up from a network of TiO_6 and PO_4 groups, linked via Ti–O–Ti, Ti–O–P, and P–O–P bonds, enclosing channels occupied by the guest rubidium cations. The structural *motif* of the framework includes isolated TiO_6 and $[Ti_2O_{11}]$ groups, interconnected by (pyro)phosphate groups. The Rb^+ cations occupying the one-dimensional channels are eightfold coordinate by oxygen atoms. $Rb_3Ti_3O(P_2O_7)(PO_4)_3$ (2 linked octahedra) and $Rb_aTi_3O_2(PO_4)_2(HPO_4)_2$ (3 linked octahedra) are considered in relation to the nonlinear optical materials $KTiOPO_4$ (KTP) and $RbTiOPO_4$ (RbTP) which contain infinite –O–Ti–O–Ti–O– chains. The typical short, "titanyl" Ti=O bond found in KTP and RbTP is barely apparent in $Rb_2Ti_3O_2(PO_4)_2(HPO_4)_2$ and $Rb_3Ti_3O(P_2O_7)(PO_4)_3$, and the poor nonlinear response of the title compounds is discussed in relation to the extended Ti/O chain structure in RbTP. Crystal data: $Rb_2Ti_3P_4O_{18}H_2$, M_r = 728.5, monoclinic, $P2_1$, a = 5.1851(4) Å, b = 16.770(2) Å, c = 8.4939(6) Å, β = 90.940(3) °, V = 738.48 Å^3, Z = 2. Final residuals of R = 4.24% and R_w = 4.40% were obtained for 2331 unique reflections with $I > 3\sigma(I)$. $Rb_3Ti_3P_5O_{20}$, M_r = 874.96, orthorhombic, $Pca2_1$, a = 18.280(1) Å, b = 6.295(1) Å, c = 14.773(1) Å, V = 1700.0 Å^3, Z = 4, R = 4.00%, and R_w = 3.70% for 1498 unique reflections with $I > 3\sigma(I)$. © 1994 Academic Press, Inc.

INTRODUCTION

The titanium(IV)-containing phase $KTiOPO_4$ (KTP) has important technological applications in such diverse areas as switching devices in telecommunications, optical computing, and laser second-harmonic generation (SHG) (1–3). The crystal structure of KTP consists of one-dimensional, corner-linked chains of octahedral TiO_6 groups, crosslinking tetrahedral phosphate groups, and irregularly coordinated univalent cations (4), in which the –Ti–O–Ti–O– backbone of the TiO_6 chains shows a characteristic short–long Ti–O bond length alternation. It is believed that the short, highly polarizable "titanyl" Ti=O double bonds play a key role in defining nonlinear optical properties (5), although they cannot be considered *in isolation* to arrive at a comprehensive structure/property relationship for all KTP-type materials (6, 7).

The optical and physical properties (8) and crystal structure (9) of the KTP-type phase rubidium titanyl phosphate, $RbTiOPO_4$, have recently been described. $RbTiOPO_4$ has very similar structural and optical properties to KTP, and shows great promise in applications as a waveguide material (10, 11). As well as $RbTiOPO_4$, the nasicon-type phase $RbTi_2(PO_4)_3$ (12) has been previously reported in the Rb/Ti/P/O phase space. This latter phase is a member of a large family of $M_2M'_2(XO_4)_3$-type materials and contains isolated TiO_6 octahedra, connected to each other via phosphate groups. The novel Ti^{III}-containing phase $RbTiP_2O_7$ was recently reported (13).

Because of the potential technological interest in phases containing octahedral $Ti^{IV}O_6$ groups, we are currently making efforts to prepare and characterize other phases in the M^+/Ti/P/O structure field: Here we report the syntheses and single crystal X-ray structures of $Rb_2Ti_3O_2(PO_4)_2(HPO_4)_2$ (Rb2Ti3P4) and $Rb_3Ti_3O(P_2O_7)(PO_4)_3$ (Rb3Ti3P5). Rb3Ti3P5 contains dimeric TiO_6 groups and Rb2Ti3P4 contains trimeric TiO_6 units, and both of these phases crystallize in noncentrosymmetric space groups, but their SHG responses are negligible. This poor optical response is briefly discussed in terms of the small number of linked TiO_6 units and small octahedral TiO_6 distortions in these phases versus the infinite, "conjugated" Ti/O chain configuration found in $KTiOPO_4$ and $RbTiOPO_4$.

[1] To whom correspondence should be addressed.

0022-4596/94 $6.00
Copyright © 1994 by Academic Press, Inc.
All rights of reproduction in any form reserved.

$Rb_3Ti_3O(P_2O_7)(PO_4)_3$ is isostructural with the recently described $K_3Ti_3P_5O_{20}$ (14).

EXPERIMENTAL

Synthesis. $Rb_2Ti_3O_2(PO_4)_2(HPO_4)_2$ was synthesized hydrothermally from starting reagents of analytical grade or better: 1.830 g RbH_2PO_4, 0.064 g TiO_2, and 0.625 cm $4M$ H_3PO_4 were sealed in a 1/4 × 3 in. gold tube and heated to 650°C in a Leco Tem-Press hydrothermal reactor. The mixture was soaked at this temperature for 60 hr, achieving an estimated pressure of 47,500 psi. The tube was then cooled to 500°C over 20 hr (cooling rate = 7.5°C/hr) and quenched to ambient temperature. Numerous transparent, rod-like crystals with maximum dimensions 0.5 × 0.5 × 2.0 mm were recovered from the tube contents by suction filtration. X-ray powder data on a well-ground sample of $Rb_2Ti_3O_2(PO_4)_2(HPO_4)_2$ (Scintag automated diffractometer, Cu$K\alpha$ radiation) indicated a complex, low-symmetry phase with a powder pattern dissimilar to those of known Rb/Ti/P/O materials. It could be successfully simulated with LAZY-PULVERIX (15) using the single-crystal structural parameters described below.

$Rb_3Ti_3O(P_2O_7)(PO_4)_3$ was prepared in single-crystal form by dissolving TiO_2 in a rubidium phosphate melt (Rb : P = 0.87–0.93) as follows: A mixture of 0.48 g TiO_2, 4.75 g RbH_2PO_4, and 0.35 g $NH_4H_2PO_4$ was thoroughly mixed dry and pre-fused at 1050°C in a platinum crucible. The final weight of the clear melt corresponded with that expected from the loss of the appropriate amounts of ammonia and water. Reheating the crucible to 1050°C for 4 hr, followed by a fast cool (4 hr) to 950°C and a slow cool (85 hr) to 850°C gave a clear syrup (removed by hot decantation) over a mass of crystals of dimensions up to 5 × 3 × 2 mm. These crystals were purified of adhering flux by washing with water to yield 0.89 g of mostly rod-shaped prisms. X-ray powder data indicated a different new phase, the powder pattern of which could be simulated using LAZY-PULVERIX.

Other phases are accessible from similar melts, the product depending on the initial Rb : P ratio in the flux: For Rb : P = 1.1 to 1.6, $RbTiOPO_4$ results; at Rb : P = 0.8, $RbTi_2(PO_4)_3$ is formed, and at Rb : P < 0.6, no rubidium-containing phases are present and only TiP_2O_7 crystals form.

Optical/spectroscopic measurements. Powder SHG data were obtained at 1.06 μ with a system based on that described earlier (16). A Kigre MK-367 Nd/YAG laser produced 20-mJ, 4-ns pulses in single-shot mode and data were collected in reflectance mode, with SHG intensity measured relative to a reference signal for quartz. The SHG response of $Rb_2Ti_3O_2(PO_4)_2(HPO_4)_2$ was ~2× that of quartz; that of $Rb_3Ti_3O(P_2O_7)(PO_4)_3$ was ~12.5× quartz, indicating that both of these materials crystallize in noncentrosymmetric space groups.

TABLE 1
Crystallographic Parameters

	$Rb_2Ti_3O_2(PO_4)_2(HPO_4)_2$	$Rb_3Ti_3O(P_2O_7)(PO_4)_3$
Empirical formula	$Rb_2Ti_3P_4O_{18}H_2$	$Rb_3Ti_3P_5O_{20}$
Formula weight	728.50	874.96
Habit	Colorless needle	Colorless prism
Crystal system	Monoclinic	Orthorhombic
a (Å)	5.1851(4)	18.280(1)
b (Å)	16.770(2)	6.295(1)
c (Å)	8.4939(6)	14.773(1)
α (°)	90	90
β (°)	90.940(3)	90
γ (°)	90	90
V (Å^3)	738.48	1700.0
Z	2	4
Space group	$P2_1$ (No. 4)	$Pca2_1$ (No. 29)
T (°C)	25(2)	23(2)
λ(Mo$K\alpha$) (Å)	0.71073	0.71073
ρ_{calc} (g/cm^3)	3.28	3.42
μ(Mo$K\alpha$) (cm^{-1})	84.7	102.4
Absorption corr.	ψ-scan	Analytical
hkl-data limits	$-7 \rightarrow 7$, $0 \rightarrow 25$, $0 \rightarrow 12$	$-8 \rightarrow 8$, $0 \rightarrow 19$, $0 \rightarrow 23$
Total data	3020	4166
Observed data[a]	2331	1498
Parameters	245	181
$R(F_o)$ (%)[b]	4.24	4.00
$R_w(F_o)$ (%)[c]	4.40	3.70

[a] $I > 3\sigma(I)$ after merging.
[b] $R = \Sigma||F_o| - |F_c||/\Sigma|F_o|$.
[c] $R_w = [\Sigma_w(|F_o| - |F_c|)^2/\Sigma_w|F_o|^2]^{1/2}$.

Crystal structure determination. For $Rb_2Ti_3O_2(PO_4)_2(HPO_4)_2$, a transparent needle-like crystal of approximate dimensions 0.3 × 0.03 × 0.02 mm was selected for data collection and mounted on a glass fiber with cyanoacrylate adhesive. Room temperature (25(2)°C) intensity data were collected on a Huber automated 4-circle diffractometer (graphite-monochromated Mo$K\alpha$ radiation, λ = 0.71073 Å) as outlined in Table 1. The unit cell and orientation matrix were established from 26 reflections which had been located and centered by searching reciprocal space ($10° < 2\theta < 22°$), and optimized by least-squares refinement, resulting in the lattice parameters shown in Table 1. Intensity data were collected in the θ-2θ scanning mode ($2\theta_{max} = 65°$) with standard reflections monitored for intensity variation throughout the course of the experiment. The scan speed was 6°/min with a scan range of 1.3° below $K\alpha_1$ to 1.6° above $K\alpha_2$. No significant variation in standards was observed, and crystal absorption was empirically corrected for using ψ-scans through 360° for selected reflections with χ near 90°. The raw data (3020 reflections) were processed using a Leh-

mann–Larsen profile-fitting routine and the normal corrections for Lorentz and polarization effects were made. All the data collection and reduction routines were based on the UCLA crystallographic computing package (17). After data reduction and merging (R_{Merge} = 1.5%), 2331 reflections were considered observable according to the criterion $I > 3\sigma(I)$. The systematic absence condition ($0k0$; k) was consistent with space groups $P2_1$ (No. 4) and $P2_1/m$ (No. 11).

The structure of $Rb_2Ti_3O_2(PO_4)(HPO_4)_2$ was solved by a combination of direct methods and Fourier syntheses, assuming the crystal structure was noncentrosymmetric $P2_1$, as confirmed by the course of the subsequent refinement, a test for "missing" crystallographic symmetry, and the nonzero second-harmonic measurement. A chemically reasonable direct-methods solution for the heavy atoms (Rb and Ti) was obtained from the program SHELXS-86 (18), and the phosphorus and oxygen atoms were located from Fourier difference maps following refinement of the known atoms positions. The least-squares, Fourier, and subsidiary calculations were performed using the Oxford CRYSTALS (19) system, running on a DEC MicroVAX-II computer. Final full-matrix refinements (245 parameters) were against F and included anisotropic temperature factors and a Larson secondary extinction correction (20). Neutral-atom scattering factors, including anomalous dispersion terms, were obtained from "International Tables" (21). The final weighting scheme was that of Tukey and Prince, using a three-term modified Chebychev polynomial fit (22), with coefficients 3.4(4), 0.0(2), and 1.2(4), resulting in R-factors of R = 4.24%, R_w = 4.50%, as defined in Table 1. Final Fourier difference maps revealed no regions of significant electron density (max = $2e/Å^3$ near O(16)), and analysis of the various trends in F_o versus F_c revealed no unusual effects. Anisotropic thermal factors and tables of observed and calculated structure factor amplitudes are available as supplementary material from the authors.

Intensity data for $Rb_3Ti_3O(P_2O_7)(PO_4)_3$ were collected on an Enraf–Nonius CAD-4 diffractometer: colorless; cut triangular prism; ~0.13 × 0.17 × 0.33 mm; refined orthorhombic lattice parameters (Table I) from 23 centered reflections; T = 23°C; graphie monochromator; Mo$K\alpha$ radiation (λ = 0.71073 Å); $2.2° < 2\theta < 55°$; ω-2θ scan mode; scan width = 1.20–1.90°; ω scan rate = 1.20–1.90°/min; data octants: +++ and −++; no variation in standards; absorption correction from numerical integration (min = 0.22, max = 0.34); 1498 unique reflections with $I > 3\sigma(I)$ after data reduction and merging; systematic absences ($0kl$, l; $h0l$, l) consistent with space groups $Pca2_1$ (No. 29) and $Pcam$ (No. 57).

The structure of $Rb_3Ti_3O(P_2O_7)(PO_4)_3$ was solved by direct methods, using the "difficult solution" option of the program MULTAN (23); the noncentrosymmetric space group was chosen for refinement based on a nonzero SHG signal observed for this phase. Refinement in the centrosymmetric space group resulted in higher R-factors and unrealistic thermal parameters. Full-matrix refinement against F; scattering factors from "International Tables"; Rb, Ti, and P refined anisotropically, O refined isotropically; extinction correction = 8.74(26) × 10^{-4} mm; weighting scheme $\propto [\sigma^2(I) + 0.00091(I)^2]^{1/2}$; 180 parameters; final R = 4.00%, R_w = 3.70%; max $\Delta/\sigma < 0.02$; problems of pseudo-symmetry between the oxygen-atom positional and thermal parameters (vide infra) precluded O-atom anisotropic refinement. Final Fourier difference maps (max = $1.2e/Å^2$ near Rb(2)) revealed no additional atomic sites. The program MISSYM (24) confirmed the pseudo-centrosymmetric nature of the structure of $Rb_3Ti_3O(P_2O_7)(PO_4)_3$, as discussed below. Anisotropic thermal factors and tables of observed and calculated structure factor amplitudes are available as supplementary material from the authors.

RESULTS

$Rb_2Ti_3O_2(PO_4)_2(HPO_4)_2$. Final atomic positional and equivalent isotropic thermal factors for $Rb_2Ti_3O_2(PO_4)_2(HPO_4)_2$ are listed in Table 2, and selected bond distance/data are presented in Tables 3 and 4. An ORTEP (25) plot of the asymmetric Ti/P/O unit and atom-labeling scheme is shown in Fig. 1. $Rb_2Ti_3O_2(PO_4)_2(HPO_4)_2$ is a three-dimensional structure containing large one-dimensional channels in the **a**-direction. There are two rubidium atoms, three Ti atoms, four P atoms, and 18 oxygen atoms in the asymmetric unit of the noncentrosymmetric unit cell. The proton positions were not located in the crystal structure study. The complete crystal structure of Rb2Ti3P4, viewed down the **a**-axis, is illustrated in Fig. 2, and with STRUPLO (26), as a polyhedral plot, in Fig. 3.

The two crystallographically distinct rubidium cations (Fig. 4) in $Rb_2Ti_3O_2(PO_4)_2(HPO_4)_2$ are both irregularly coordinated to eight oxygen atoms within 3.3 Å (d_{av}[Rb(1)–O] = 3.139(5) Å, d_{av}[Rb(2)–O] = 3.131(4) Å). These average distances are significantly larger than the ionic-radius sum for Rb^+ and O^{2-} which is ~3.03 Å (27). Selecting a cutoff distance for Rb–O interactions can be problematical: if the bonding sphere around each Rb^+ cation is increased to 3.55 Å, the oxygen coordination of both Rb^+ species increases to 12. In this latter case, the longest Rb–O contact considered to be a bonding interaction yields a bond valence (28) of 0.04; by comparison, the closest Rb–P contact is 3.6 Å. The value of 3.3 Å was chosen for comparability with that used in the $Rb_3Ti_3O(P_2O_7)(PO_4)_3$ structure reported below.

The three titanium atoms all make contact with six oxygen atom neighbors in octahedral coordination [d_{av}

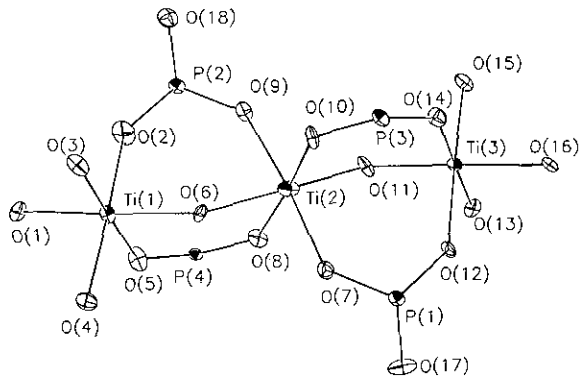

FIG. 1. ORTEP view of the asymmetric unit of $Rb_2Ti_3O_2(PO_4)_2(HPO_4)_2$, showing the atom-labeling scheme (Rb cations omitted). 50% thermal ellipsoids.

TABLE 2
Atomic Positional and Thermal Parameters for $Rb_2Ti_3O_2(PO_4)_2(HPO_4)_2$

Atom	x	y	z	U_{eq}[a]
Rb(1)	0.4168(4)	0.3983(2)	0.8966(2)	0.0252
Rb(2)	0.0779(4)	0.1369(2)	0.6055(2)	0.0250
Ti(1)	0.4436(5)	0.4417(2)	0.4128(3)	0.0096
Ti(2)	0.7635(7)	0.2660(3)	0.2436(5)	0.0127
Ti(3)	1.0535(5)	0.0980(2)	0.0878(3)	0.0079
P(1)	0.5474(6)	0.1821(3)	−0.0765(5)	0.0084
P(2)	0.9510(7)	0.3551(3)	0.5728(5)	0.0090
P(3)	0.5727(6)	0.0871(3)	0.3247(5)	0.0089
P(4)	0.9201(7)	0.4510(3)	0.1740(4)	0.0079
O(1)	0.442(2)	0.5476(7)	0.515(1)	0.0103
O(2)	0.729(2)	0.4150(8)	0.549(2)	0.0135
O(3)	0.214(2)	0.3992(7)	0.570(1)	0.0121
O(4)	0.154(2)	0.4738(9)	0.280(1)	0.0152
O(5)	0.670(2)	0.4813(7)	0.255(1)	0.0144
O(6)	0.467(2)	0.3365(7)	0.316(1)	0.0090
O(7)	0.564(2)	0.2466(7)	0.054(1)	0.0137
O(8)	0.909(2)	0.3614(7)	0.145(1)	0.0102
O(9)	0.950(2)	0.2933(7)	0.442(1)	0.0113
O(10)	0.592(2)	0.1781(7)	0.351(1)	0.0116
O(11)	1.021(2)	0.1978(7)	0.180(1)	0.0121
O(12)	0.774(2)	0.1245(7)	−0.056(1)	0.0105
O(13)	1.297(2)	0.1367(8)	−0.069(1)	0.0097
O(14)	0.809(2)	0.0561(7)	0.241(1)	0.0128
O(15)	1.334(2)	0.0678(7)	0.227(1)	0.0126
O(16)	1.061(2)	−0.0089(7)	−0.012(1)	0.0102
O(17)	0.562(2)	0.2236(9)	−0.238(2)	0.0173
O(18)	0.932(2)	0.3153(7)	0.732(2)	0.0158

[a] U_{eq} (Å^2) = $(U_1U_2U_3)^{1/3}$.

(Ti(1)–O) = 1.940(5) Å, d_{av}(Ti(2)–O) = 1.954(5) Å, d_{av} (Ti(3)–O) = 1.937(5) Å] and the four phosphorus atoms all show typical tetrahedral oxygen-atom coordination, with d_{av} values of 1.533(7), 1.531(7), 1.523(6), and 1.542(6) Å for P(1), P(2), P(3), and P(4), respectively. The 18 oxygen atoms break down into several groups, depending on their coordination: O(1), O(8), O(10), and O(16) bond to two rubidium atoms, one titanium atom, and one phosphorus atom; O(2), O(3), O(4), O(5), O(7), O(9), O(12), O(13), O(14), and O(15) bond to 1 Rb, 1 Ti, and 1 P; O(6) and O(11) bridge two titanium atoms; and the protonated O(17) and O(18) are each in contact with 3 Rb and 1 P.

The building block of the structure consists of isolated groups of three vertex-sharing TiO_6 octahedra (Fig. 1), forming a "trimeric" $[Ti_3O_{16}]$ unit. The linkage of the central TiO_6 octahedron is almost exactly *trans* with re-

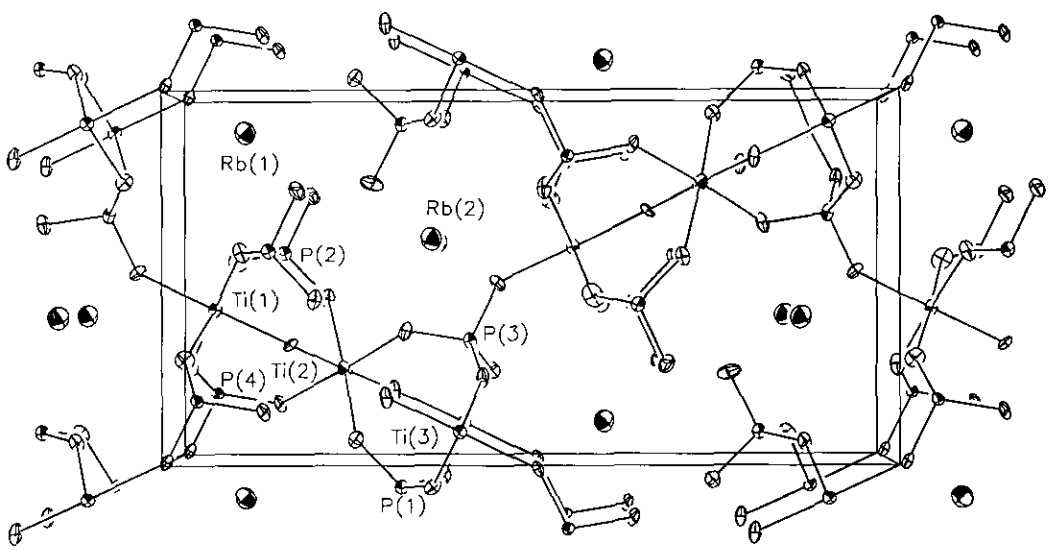

FIG. 2. View down a of the crystal structure of $Rb_2Ti_3O_2(PO_4)_2(HPO_4)_2$, with selected nonoxygen atoms labeled. 50% thermal ellipsoids.

TABLE 3
Bond Distances (Å) for $Rb_2Ti_3O_2(PO_4)_2(HPO_4)_2$

Rb(1)–O(3)	2.95(1)	Rb(1)–O(7)	2.97(1)
Rb(1)–O(14)	3.11(1)	Rb(1)–O(15)	3.30(2)
Rb(1)–O(16)	3.10(1)	Rb(1)–O(16)	3.26(1)
Rb(1)–O(17)	3.24(2)	Rb(1)–O(18)	3.18(1)
Rb(2)–O(1)	3.23(1)	Rb(2)–O(1)	3.09(1)
Rb(2)–O(4)	3.15(1)	Rb(2)–O(5)	3.14(1)
Rb(2)–O(9)	3.03(1)	Rb(2)–O(13)	2.97(1)
Rb(2)–O(17)	3.17(1)	Rb(2)–O(18)	3.27(1)
Ti(1)–O(1)	1.98(1)	Ti(1)–O(2)	1.92(1)
Ti(1)–O(3)	1.94(1)	Ti(1)–O(4)	1.94(1)
Ti(1)–O(5)	1.91(1)	Ti(1)–O(6)	1.95(1)
Ti(2)–O(6)	2.04(1)	Ti(2)–O(7)	1.93(1)
Ti(2)–O(8)	1.96(1)	Ti(2)–O(9)	1.98(1)
Ti(2)–O(10)	1.95(1)	Ti(2)–O(11)	1.84(1)
Ti(3)–O(11)	1.86(1)	Ti(3)–O(12)	1.93(1)
Ti(3)–O(13)	1.96(1)	Ti(3)–O(14)	1.96(1)
Ti(3)–O(15)	1.93(1)	Ti(3)–O(16)	1.98(1)
P(1)–O(7)	1.55(1)	P(1)–O(12)	1.53(1)
P(1)–O(13)	1.51(1)	P(1)–O(17)	1.54(1)
P(2)–O(2)	1.54(1)	P(2)–O(3)	1.55(1)
P(2)–O(9)	1.52(1)	P(2)–O(18)	1.51(1)
P(3)–O(1)	1.52(1)	P(3)–O(10)	1.55(1)
P(3)–O(14)	1.52(1)	P(3)–O(15)	1.51(1)
P(4)–O(4)	1.54(1)	P(4)–O(5)	1.56(1)
P(4)–O(8)	1.52(1)	P(4)–O(16)	1.54(1)

TABLE 4
Selected Bond Angles (°) for $Rb_2Ti_3O_2(PO_4)_2(HPO_4)_2$

O(2)–Ti(1)–O(1)	87.5(5)	O(3)–Ti(1)–O(1)	91.2(5)
O(3)–Ti(1)–O(2)	88.7(5)	O(4)–Ti(1)–O(1)	89.8(5)
O(4)–Ti(1)–O(2)	177.3(6)	O(4)–Ti(1)–O(3)	91.4(5)
O(5)–Ti(1)–O(1)	90.1(5)	O(5)–Ti(1)–O(2)	91.4(5)
O(5)–Ti(1)–O(3)	178.6(6)	O(5)–Ti(1)–O(4)	88.6(5)
O(6)–Ti(1)–O(1)	176.6(5)	O(6)–Ti(1)–O(2)	89.4(6)
O(6)–Ti(1)–O(3)	90.0(5)	O(6)–Ti(1)–O(4)	93.3(6)
O(6)–Ti(1)–O(5)	88.7(5)		
O(7)–Ti(2)–O(6)	87.4(5)	O(8)–Ti(2)–O(6)	87.3(5)
O(8)–Ti(2)–O(7)	89.0(5)	O(9)–Ti(2)–O(6)	88.3(5)
O(9)–Ti(2)–O(7)	175.4(7)	O(9)–Ti(2)–O(8)	89.5(5)
O(10)–Ti(2)–O(6)	86.9(5)	O(10)–Ti(2)–O(7)	91.4(6)
O(10)–Ti(2)–O(8)	174.1(7)	O(10)–Ti(2)–O(9)	89.8(5)
O(11)–Ti(2)–O(6)	177.0(7)	O(11)–Ti(2)–O(7)	91.8(5)
O(11)–Ti(2)–O(8)	95.6(5)	O(11)–Ti(2)–O(9)	92.6(5)
O(11)–Ti(2)–O(10)	90.3(5)		
O(12)–Ti(3)–O(11)	89.3(5)	O(13)–Ti(3)–O(11)	93.1(5)
O(13)–Ti(3)–O(12)	88.7(5)	O(14)–Ti(3)–O(11)	88.7(5)
O(14)–Ti(3)–O(12)	90.9(5)	O(14)–Ti(3)–O(13)	178.2(5)
O(15)–Ti(3)–O(11)	92.8(5)	O(15)–Ti(3)–O(12)	177.8(5)
O(16)–Ti(3)–O(13)	90.9(5)	O(15)–Ti(3)–O(14)	89.4(5)
O(16)–Ti(3)–O(11)	175.9(5)	O(16)–Ti(3)–O(12)	87.6(5)
O(16)–Ti(3)–O(13)	89.5(5)	O(16)–Ti(3)–O(14)	88.7(5)
O(16)–Ti(3)–O(15)	90.3(5)		
O(12)–P(1)–O(7)	109.1(6)	O(13)–P(1)–O(7)	111.2(6)
O(13)–P(1)–O(12)	109.7(7)	O(17)–P(1)–O(7)	108.5(8)
O(17)–P(1)–O(12)	109.5(7)	O(17)–P(1)–O(13)	108.7(7)
O(3)–P(2)–O(2)	109.9(7)	O(9)–P(2)–O(2)	110.9(7)
O(9)–P(2)–O(3)	107.7(6)	O(18)–P(2)–O(2)	110.3(7)
O(18)–P(2)–O(3)	107.2(7)	O(18)–P(2)–O(9)	110.7(7)
O(10)–P(3)–O(1)	107.7(7)	O(14)–P(3)–O(1)	109.0(6)
O(14)–P(3)–O(10)	110.8(6)	O(15)–P(3)–O(1)	110.3(6)
O(15)–P(3)–O(10)	110.0(7)	O(15)–P(3)–O(14)	109.1(7)
O(5)–P(4)–O(4)	108.0(7)	O(8)–P(4)–O(4)	111.6(8)
O(8)–P(4)–O(5)	111.3(6)	O(16)–P(4)–O(4)	110.7(6)
O(16)–P(4)–O(5)	108.5(6)	O(16)–P(4)–O(8)	106.8(6)
P(3)–O(1)–Ti(1)	141.8(8)	P(2)–O(2)–Ti(1)	143.3(9)
P(2)–O(3)–Ti(1)	137.4(8)	P(4)–O(4)–Ti(1)	149.6(10)
P(4)–O(5)–Ti(1)	136.0(8)	P(2)–O(6)–Ti(1)	134.6(6)
P(1)–O(7)–Ti(2)	137.6(8)	P(4)–O(8)–Ti(2)	138.4(7)
P(2)–O(9)–Ti(2)	140.7(8)	P(3)–O(10)–Ti(2)	134.8(7)
P(3)–O(11)–Ti(2)	138.9(7)	P(1)–O(12)–Ti(3)	141.5(7)
P(1)–O(13)–Ti(3)	139.6(7)	P(3)–O(14)–Ti(3)	136.5(8)
P(3)–O(15)–Ti(3)	151.9(9)	P(4)–O(16)–Ti(3)	141.4(7)

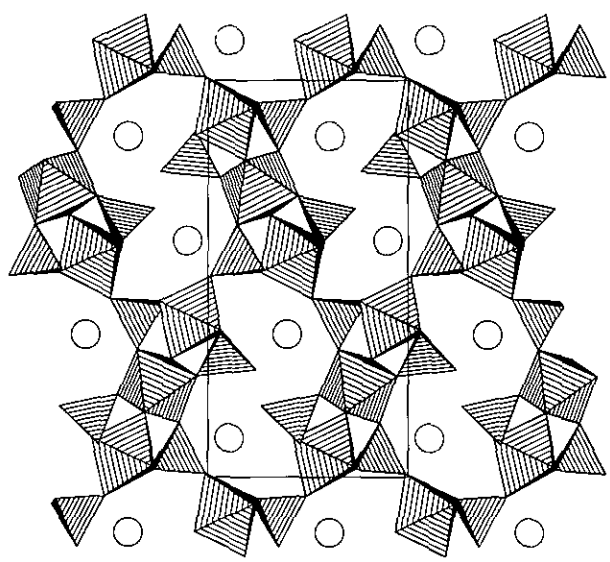

FIG. 3. Polyhedral plot of the crystal structure of $Rb_2Ti_3O_2(PO_4)_2(HPO_4)_2$, viewed down the **a**-direction, showing the one-dimensional channels occupied by Rb^+ cations (drawn as circles of arbitrary size).

spect to its two TiO_6 neighbors [θ(O(6)–Ti(2)–O(11)) = 177.0(7)°]. The bridging-oxygen angles are typical of those found in KTP-type materials (6, 7, 9). θ[Ti(1)–O(6)–Ti(2)] = 134.6(6)°; θ[Ti(2)–O(11)–Ti(3)] = 139.0(7)°. The remaining 14 oxygen vertices of the trimer form Ti–O–P bond (θ_{av} = 141°). The Ti(1) octahedron is the most regular of the three: defining octahedral displacement (or Ti–oxygen-atom-barycenter distance) as

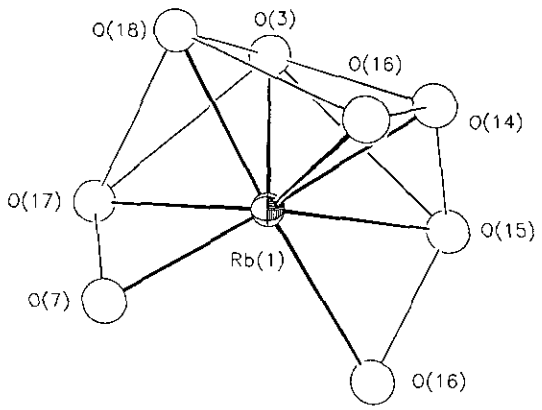

FIG. 4. Typical Rb-cation environment in $Rb_2Ti_3O_2(PO_4)_2(HPO_4)_2$, showing Rb–O bonds, and O · · · O contacts < 4.2 Å (thin lines).

$$\Delta = r(\mathrm{Ti}) - \frac{1}{6}\Sigma r(\mathrm{O}),$$

where r are orthogonal atomic coordinates, and the summation is over the six octahedral nearest-neighbor oxygens, $\Delta(\mathrm{Ti}(1)) = 0.018$ Å. Notably, there is no identifiable, short ($d < 1.8$ Å) "titanyl" Ti=O bond, as found in $RbTiOPO_4$ (29). The corresponding Δ values for the Ti(2) (most distorted) and Ti(3) octahedra are 0.093 and 0.049 Å, respectively. These values are further discussed below.

All four phosphate groups are involved in bridging Ti–O–P linkages: two of the four PO_4 groups [P(3) and P(4)] make 4 of these bonds, while the other two [P(1) and P(2)] make three bonds to Ti via O and also have an uncoordinated P–OH vertex. $P(3)O_4$ and $P(4)O_4$ each use two of their vertices to make a bridging link over two of the octahedra in the Ti_3O_{16} trimer, resulting, in Ti–P–Ti "3-rings" (oxygen designations omitted). The other two oxygen atoms link to adjacent Ti_3O_{16} units: one link in the **bc**-plane forming sheets, and one link to similar units in the **a**-direction, forming columns. The $P(1)O_4$ and $P(2)O_4$ groups also make an *intra*-titanyl trimer bridge and an *inter*-layer P–O–Ti link. The fourth –OH vertex of these tetrahedra points into the channel region, and possibly forms a P–OH · · · (H)O–P hydrogen bond: the O(17) · · · O(18) nonbonding contact of 2.48 Å is short.

The atomic coordinates of $Rb_2Ti_3O_2(PO_4)_2(HPO_4)_2$ were input to the program MISSYM (24) which checks a given model for "missing" (unmodeled) crystallographic symmetry. MISSYM did not detect a possible center of symmetry if the atoms were allowed to be displaced by up to 1 Å from their observed positions, thus $Rb_2Ti_3O_2(PO_4)_2(HPO_4)_2$ does not appear to crystallize in a ferroelectric or other distortion from a centrosymmetric prototype phase.

TABLE 5
Atomic Positional and Thermal Parameters for $Rb_3Ti_3O(P_2O_7)(PO_4)_3$

Atom	x	y	z	$U_{eq}{}^a/U_{iso}$
Rb(1)	0.67497(6)	0.1558(2)	0.25[b]	0.024[a]
Rb(2)	0.3455(1)	0.8691(4)	0.4743(2)	0.018[a]
Rb(3)	0.3505(1)	0.8647(4)	0.0285(2)	0.019[a]
Ti(1)	0.8526(1)	0.7527(3)	0.2475(3)	0.006[a]
Ti(2)	0.5505(1)	0.7450(8)	0.1378(2)	0.008[a]
Ti(3)	0.5446(1)	0.7413(7)	0.3749(2)	0.005[a]
P(1)	0.3972(1)	0.7442(4)	0.2504(3)	0.007[a]
P(2)	0.9902(2)	0.7544(11)	0.4040(3)	0.007[a]
P(3)	1.0021(2)	0.7546(12)	0.1074(3)	0.007[a]
P(4)	0.7227(2)	0.6440(9)	0.4000(3)	0.008[a]
P(5)	0.7267(2)	0.6456(9)	0.0913(3)	0.007[a]
O(1)	0.8484(3)	0.4532(10)	0.2499(11)	0.011(2)
O(2)	0.8449(3)	1.0660(10)	0.2468(9)	0.009(2)
O(3)	0.9325(5)	0.758(2)	0.1661(6)	0.013(3)
O(4)	0.9189(5)	0.763(2)	0.3509(6)	0.013(3)
O(5)	0.7871(4)	0.7609(14)	0.1408(6)	0.010(2)
O(6)	0.7649(4)	0.7573(13)	0.3252(6)	0.011(2)
O(7)	0.4451(6)	0.749(3)	0.1653(6)	0.009(3)
O(8)	0.5278(5)	0.758(3)	0.0043(6)	0.013(3)
O(9)	0.5704(3)	0.7482(10)	0.2578(8)	0.010(2)
O(10)	0.6542(5)	0.7613(19)	0.1145(6)	0.010(3)
O(11)	0.5480(5)	0.4394(19)	0.1317(7)	0.013(3)
O(12)	0.5500(5)	1.0530(18)	0.1319(7)	0.008(3)
O(13)	0.4415(6)	0.744(3)	0.3374(6)	0.009(3)
O(14)	0.5161(6)	0.755(3)	0.5078(6)	0.013(3)
O(15)	0.6477(5)	0.7464(19)	0.4108(6)	0.013(3)
O(16)	0.5368(6)	0.4414(19)	0.3807(7)	0.011(3)
O(17)	0.5393(6)	1.0544(20)	0.3809(7)	0.013(3)
O(18)	0.7341(4)	0.7251(12)	−0.0119(5)	0.011(2)
O(19)	0.7284(5)	0.411(3)	0.0975(7)	0.016(3)
O(20)	0.7214(5)	0.4096(19)	0.3972(7)	0.011(3)

[a] $U_{eq}(\text{Å}^2) = (U_1U_2U_3)^{1/3}$.
[b] Coordinate fixed to define origin with respect to polar axis.

$Rb_3Ti_3O(P_2O_7)(PO_4)_3$. Atomic positional and heavy-atom equivalent/oxygen isotropic thermal parameters for $Rb_3Ti_3O(P_2O_7)(PO_4)_3$ are listed in Table 5, with selected geometrical data in Tables 6 and 7. $Rb_3Ti_3O(P_2O_7)(PO_4)_3$ consists of a three-dimensional octahedral/tetrahedral network surrounding one-dimensional channels occupied by the guest cations. The atomic basis in Rb3Ti3P5 consists of three rubidium atoms (eightfold oxygen coordination with $d_{max}(\mathrm{Rb–O}) = 3.3$ Å), three titanium atoms (octahedral coordination), five phosphorus atoms (tetrahedral), and 20 oxygen atoms, as illustrated in Fig. 5. The complete crystal structure of Rb3Ti3P5, viewed down the [010]-direction, is illustrated with ORTEP in Fig. 6, and with STRUPLO in Fig. 7.

The three Rb^+ cations (e.g., Fig. 8) are each located in approximate square-antiprismatic coordination, with average Rb–O contacts of $d_{av}(\mathrm{Rb(1)–O}) = 3.086(4)$ Å, $d_{av}(\mathrm{Rb(2)–O}) = 3.042(4)$ Å, and $d_{av}(\mathrm{Rb(3)–O}) = 3.048(4)$ Å.

TABLE 6
Selected Bond Distances (Å) for $Rb_2Ti_3O(P_2O_7)(PO_4)_3$

Rb(1)–O(2)	3.158(6)	Rb(1)–O(6)	3.197(8)
Rb(1)–O(9)	3.201(6)	Rb(1)–O(10)	3.212(11)
Rb(1)–O(12)	2.947(10)	Rb(1)–O(17)	3.210(11)
Rb(1)–O(19)	2.934(11)	Rb(1)–O(20)	2.829(11)
Rb(2)–O(4)	3.239(11)	Rb(2)–O(10)	3.115(11)
Rb(2)–O(12)	3.052(9)	Rb(2)–O(13)	2.791(11)
Rb(2)–O(14)	3.238(10)	Rb(2)–O(18)	2.947(8)
Rb(2)–O(19)	2.870(11)	Rb(2)–O(20)	3.086(11)
Rb(3)–O(2)	3.256(14)	Rb(3)–O(5)	3.106(9)
Rb(3)–O(7)	2.760(10)	Rb(3)–O(8)	3.330(10)
Rb(3)–O(15)	3.003(11)	Rb(3)–O(17)	3.012(10)
Rb(3)–O(19)	3.003(11)	Rb(3)–O(20)	2.911(11)
Ti(1)–O(1)	1.887(7)	Ti(1)–O(2)	1.977(6)
Ti(1)–O(3)	1.891(9)	Ti(1)–O(4)	1.952(9)
Ti(1)–O(5)	1.980(8)	Ti(1)–O(6)	1.973(8)
Ti(2)–O(7)	1.969(10)	Ti(2)–O(8)	2.017(9)
Ti(2)–O(9)	1.809(12)	Ti(2)–O(10)	1.929(8)
Ti(2)–O(11)	1.927(14)	Ti(2)–O(12)	1.941(13)
Ti(3)–O(9)	1.794(12)	Ti(3)–O(13)	1.964(11)
Ti(3)–O(14)	2.033(9)	Ti(3)–O(15)	1.957(9)
Ti(3)–O(16)	1.895(13)	Ti(3)–O(17)	1.975(14)
P(1)–O(1)	1.530(7)	P(1)–O(2)	1.531(6)
P(1)–O(7)	1.532(10)	P(1)–O(13)	1.520(10)
P(2)–O(4)	1.522(9)	P(2)–O(8)	1.517(9)
P(2)–O(16)	1.537(13)	P(2)–O(17)	1.539(13)
P(3)–O(3)	1.540(9)	P(3)–O(11)	1.525(13)
P(3)–O(12)	1.538(13)	P(3)–O(14)	1.509(9)
P(4)–O(6)	1.525(9)	P(4)–O(15)	1.523(10)
P(4)–O(18)	1.606(9)	P(4)–O(20)	1.476(12)
P(5)–O(5)	1.511(9)	P(5)–O(10)	1.551(10)
P(5)–O(18)	1.611(6)	P(5)–O(19)	1.483(13)

TABLE 7
Selected Bond Angles (Å) for $Rb_2Ti_3O(P_2)O_7)(PO_4)_3$

O(1)–Ti(1)–O(2)	173.5(3)	O(1)–Ti(1)–O(3)	93.5(5)
O(1)–Ti(1)–O(4)	92.5(6)	O(1)–Ti(1)–O(5)	90.9(5)
O(1)–Ti(1)–O(6)	88.3(4)	O(2)–Ti(1)–O(3)	92.0(5)
O(2)–Ti(1)–O(4)	90.9(5)	O(2)–Ti(1)–O(5)	85.8(4)
O(2)–Ti(1)–O(6)	86.0(4)	O(3)–Ti(1)–O(4)	91.0(3)
O(3)–Ti(1)–O(5)	87.7(4)	O(3)–Ti(1)–O(6)	175.7(4)
O(4)–Ti(1)–O(5)	176.5(4)	O(4)–Ti(1)–O(6)	92.8(4)
O(5)–Ti(1)–O(6)	88.3(4)		
O(7)–Ti(2)–O(8)	90.0(4)	O(7)–Ti(2)–O(9)	89.7(3)
O(7)–Ti(2)–O(10)	176.0(6)	O(7)–Ti(2)–O(11)	89.9(6)
O(7)–Ti(2)–O(12)	89.6(6)	O(8)–Ti(2)–O(9)	177.1(6)
O(8)–Ti(2)–O(10)	91.5(4)	O(8)–Ti(2)–O(11)	89.4(5)
O(8)–Ti(2)–O(12)	85.2(5)	O(9)–Ti(2)–O(10)	88.7(4)
O(9)–Ti(2)–O(11)	93.5(4)	O(9)–Ti(2)–O(12)	91.9(4)
O(10)–Ti(2)–O(11)	93.9(5)	O(10)–Ti(2)–O(12)	86.8(5)
O(11)–Ti(2)–O(12)	174.5(4)		
O(9)–Ti(3)–O(13)	88.8(3)	O(9)–Ti(3)–O(14)	176.2(5)
O(9)–Ti(3)–O(15)	90.5(3)	O(9)–Ti(3)–O(16)	95.0(4)
O(9)–Ti(3)–O(17)	91.9(4)	O(13)–Ti(3)–O(14)	91.5(4)
O(13)–Ti(3)–O(15)	178.5(6)	O(13)–Ti(3)–O(16)	87.0(6)
O(13)–Ti(3)–O(17)	87.6(6)	O(14)–Ti(3)–O(15)	89.1(4)
O(14)–Ti(3)–O(16)	88.8(5)	O(14)–Ti(3)–O(17)	84.4(5)
O(15)–Ti(3)–O(16)	94.4(5)	O(15)–Ti(3)–O(17)	91.1(5)
O(16)–Ti(3)–O(17)	171.1(4)		
O(1)–P(1)–O(2)	105.6(4)	O(1)–P(1)–O(7)	110.1(8)
O(1)–P(1)–O(13)	108.3(9)	O(2)–P(1)–O(7)	108.3(8)
O(2)–P(1)–O(13)	111.3(8)	O(7)–P(1)–O(13)	112.9(3)
O(4)–P(2)–O(8)	108.5(5)	O(4)–P(2)–O(16)	112.7(7)
O(4)–P(2)–O(17)	110.9(7)	O(8)–P(2)–O(16)	110.5(7)
O(8)–P(2)–O(17)	109.4(7)	O(16)–P(2)–O(17)	104.8(5)
O(3)–P(3)–O(11)	109.5(7)	O(3)–P(3)–O(12)	109.1(7)
O(3)–P(3)–O(14)	111.6(6)	O(11)–P(3)–O(12)	105.2(5)
O(11)–P(3)–O(14)	110.6(7)	O(12)–P(3)–O(14)	110.8(7)
O(6)–P(4)–O(15)	109.5(6)	O(6)–P(4)–O(18)	100.9(5)
O(6)–P(4)–O(20)	117.0(6)	O(15)–P(4)–O(18)	103.0(5)
O(15)–P(4)–O(20)	114.4(6)	O(18)–P(4)–O(20)	110.3(6)
O(5)–P(5)–O(10)	107.0(6)	O(5)–P(5)–O(18)	104.4(5)
O(5)–P(5)–O(19)	115.7(6)	O(10)–P(5)–O(18)	97.7(5)
O(10)–P(5)–O(19)	118.3(6)	O(18)–P(5)–O(19)	111.5(5)
Ti(1)–O(1)–P(1)	142.0(4)	Ti(1)–O(2)–P(1)	137.2(4)
Ti(1)–O(3)–P(3)	174.5(6)	Ti(1)–O(4)–P(2)	159.1(6)
Ti(11)–O(5)–P(5)	144.6(6)	Ti(1)–O(6)–P(4)	145.7(5)
Ti(12)–O(6)–P(1)	136.8(6)	Ti(2)–O(8)–P(2)	177(1)
Ti(2)–O(9)–Ti(3)	153.1(4)	Ti(2)–O(10)–P(5)	148.7(8)
Ti(12)–O(11)–P(3)	145.5(7)	Ti(2)–O(12)–P(3)	143.1(6)
Ti(13)–O(13)–P(1)	138.6(6)	Ti(3)–O(14)–P(3)	176.7(9)
Ti(13)–O(15)–P(4)	146.2(7)	Ti(3)–O(16)–P(2)	148.3(7)
Ti(13)–O(17)–P(2)	145.0(7)	P(4)–O(18)–P(5)	135.2(5)

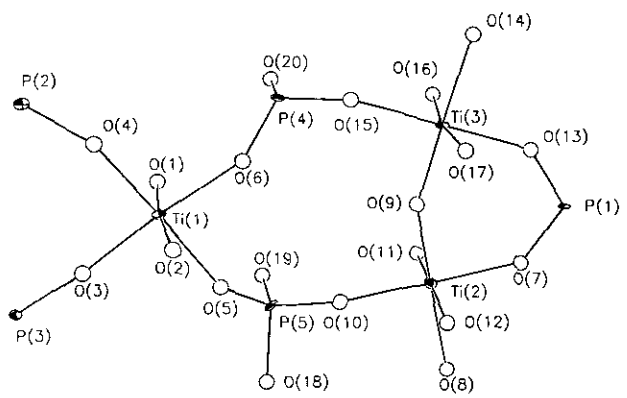

FIG. 5. ORTEP view of the asymmetric unit of $Rb_3Ti_3O(P_2O_7)(PO_4)_3$, showing the atom-labeling scheme, omitting the Rb^+ species. 50% thermal factors.

Each average distance is slightly larger than the average Rb–O ionic-radii-sum contact noted above. The closest Rb–P contact is >3.5 Å, although this is "shielded" by oxygen atoms. The titanium/oxygen octahedra each show typical average bond distances: d_{av}(Ti(1)–O) =

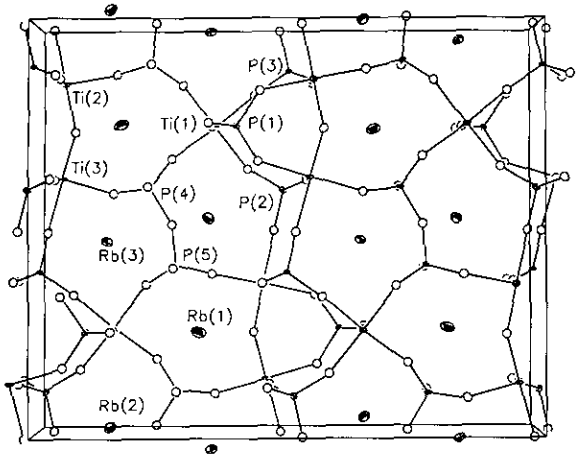

FIG. 6. View down **b** of the crystal structure of $Rb_3Ti_3O(P_2O_7)(PO_4)_3$, with selected nonoxygen atoms labeled. 50% thermal factors.

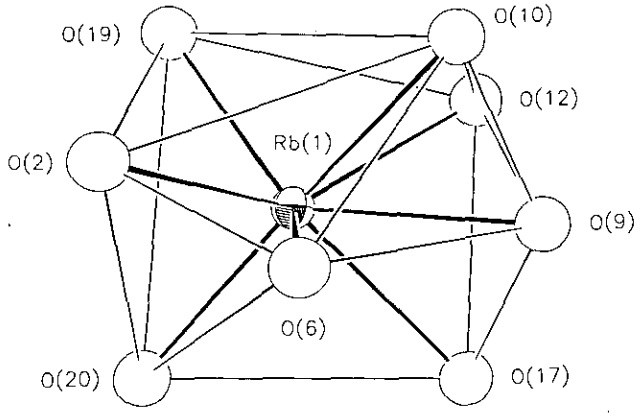

FIG. 8. Rb(1) cation environment in $Rb_3Ti_3O(P_2O_7)(PO_4)_3$, with Rb–O bonds indicated by thick lines, and O · · · O contacts < 4.5 Å indicated by thin lines.

1.943(4) Å, d_{av}(Ti(2)–O) = 1.932(5) Å, and d_{av}(Ti(3)–O) = 1.936(5) Å. O–Ti–O *cis* bond angles are all within the range 84–95°. There are three phosphate groups present in the structure, each showing typical geometrical behavior: d_{av}(P(1)–O) = 1.528(5) Å, d_{av}(P(2)–O) = 1.529(6) Å, and d_{av}(P(3)–O) = 1.528(6) Å. The two remaining P-atoms [P(4) and P(5)] are part of a P_2O_7 pyrophosphate group, and the P–O bonds to the linking oxygen atom, O(18), are typically extended (d_{av} = 1.609(7) Å), as found in other P_2O_7 groups (30). Both these P-atoms also bond to an "unsaturated" oxygen atom, as P(4)–O(19) and P(5)–O(20), respectively, not linked to any other species, with d_{av} = 1.480(9) Å. The 20 oxygen atoms may be classified according to their nearest neighbor Ti/P species: one oxygen atom, O(9), bridges two titanium atoms, with θ[Ti(2)–O(9)–Ti(3)] = 153.1(4)° substantially larger than the values for $Rb_2Ti_3O_2(PO_4)_2(HPO_4)_2$ reported above. One O-atom, O(18), links two phosphorus atoms in the pyrophosphate group, with θ[P(4)–O(18)–P(5)] = 135.2(5)°. The other 16 oxygen atoms [O(1) to O(8), O(10) to O(17)] form Ti–O–P bridges. Three of these links, Ti(1)–(3)–P(3), Ti(2)—O(8)–P(2), and Ti(3)–O(14)–P(3), are almost linear (Table 6). The average bond angle of the remainder is θ_{ave}(Ti–O–P) = 144.7(4)°.

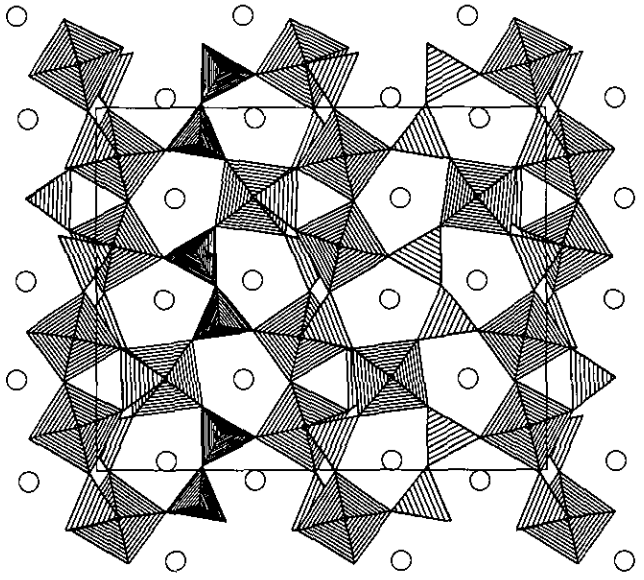

FIG. 7. Polyhedral plot of the crystal structure of $Rb_3Ti_3O(P_2O_7)(PO_4)_3$, viewed down the **b**-direction.

Unlike the situation in $Rb_2Ti_3O_2(PO_4)_2(HPO_4)_2$, the three crystallographically distinct titanium atoms in $Rb_3Ti_3O(P_2O_7)(PO_4)_3$ are not linked into a single unit, but form an isolated TiO_6 unit [titanium atom Ti(1)] and a "dimeric" Ti_2O_{11} group [Ti(2) and Ti(3)]. Ti-atom octahedral distortions, Δ, defined as above, are 0.074, 0.069, and 0.082 Å for Ti(1), Ti(2), and Ti(3) respectively. Both the phosphate and pyrophosphate groups are involved in linking the TiO_6/Ti_2O_{11} units into a complex three-dimensional network. The most notable feature of the structure is the presence of one-dimensional channels which propagate in the polar **c**-direction of the structure (Fig. 7).

The use of the program MISSYM confirmed that the atomic coordinates in space group $Pca2_1$ of $Rb_3Ti_3O(P_2O_7)(PO_4)_3$ are pseudo-centrosymmetric with respect to a mirror plane at z = 1/4 (i.e., space group *Pcam*). The maximum atomic displacement from the centrosymmetric prototype symmetry was ~0.35 Å for some of the oxygen atoms. Notably, all the heavy atoms, including the Rb^+ species, lie within 0.1 Å of their potential *Pcam* positions.

DISCUSSION

The two new titanium(IV)-containing phases $Rb_2Ti_3O_2(PO_4)_2(HPO_4)_2$ and $Rb_3Ti_3O(P_2O_7)(PO_4)_3$ described above

both crystallize in noncentrosymmetric space groups, but their powder SHG responses are negligible compared to that of $RbTiOPO_4$ and other KTP-type materials. It is therefore useful to compare these new structures with that formed by KTP-type materials, to detect if any structural differences may be correlated with the exceptional optical properties of the KTP family.

It is immediately apparent that the criterion of crystallizing in a noncentrosymmetric space group is insufficient to guarantee a substantial SHG response, even in these materials which contain the same atomic species as those found in $RbTiOPO_4$, including the "favored" octahedral $Ti^{IV}O_6$ group (5). Although $Rb_3Ti_3O(P_2O_7)(PO_4)_3$ is pseudo-centrosymmetric, and might a priori be expected to have a relatively small SHG response, $Rb_2Ti_3O_2(PO_4)_2(HPO_4)_2$ apparently cannot transform to a centrosymmetric prototype modification, but its SHG response is much less than that of KTP types. Conversely, many KTP-type phases do show a ferroelectric–paraelectric phase transition (31) (space group transformation $Pna2_1 \rightarrow Pnan$ as demonstrated for $TlTiOPO_4$) (32), and it has been shown that the Ti/P/O-framework of KTP-type materials is close (within ~0.2 Å) to being centrosymmetric (9). This typical KTP-framework distortion is *less* than that observed for the T/P/O-atoms in $Rb_3Ti_3O(P_2O_7)(PO_4)_3$, as reported above, although the *guest cation* in KTP types can often be displaced by as much as 0.75 Å from its potential centrosymmetric site, while the Rb cations in $Rb_3Ti_3O(P_2O_7)(PO_4)_3$ are displaced by very small distances from their potential centrosymmetric sites.

Further similarity between these three structures ($Rb_2Ti_3O_2(PO_4)_2(HPO_4)_2$, $Rb_3Ti_3O(P_2O_7)(PO_4)_3$, and $RbTiOPO_4$) is shown by the fact that they are built up from the same polyhedral units (TiO_6 octahedra and PO_4 tetrahedra) and these moieties are linked by Ti–O–Ti as well as Ti–O–P bonds (and a P–O–P bond in $Rb_3Ti_3O(P_2O_7)(PO_4)_3$). KTP-type materials contain *infinite* chains of vertex-sharing titanium/oxygen octahedra, bonding alternately *cis* and *trans* to each other (4), which may be written as $O–[TiO_5]_n$, with $n = \infty$. In Rb3Ti3P5, $n = 2$ for the Ti_2O_{11} grouping, and in Rb2Ti3P4, n is limited to 3 for one Ti_3O_{16} "chain" unit. Thus, the Ti_2O_{11} dimer in $Rb_3Ti_3O(P_2O_7)(PO_4)_3$ and, in particular, the Ti_3O_{16} trimer in $Rb_2Ti_3O_2(PO_4)_2(HPO_4)_2$, are closely related to a subunit of the infinite chain in KTP-type phases. However, their local symmetries are distinct: In particular, in Rb2Ti3P4 the Ti_3O_{16} unit is *pseudo*-centrosymmetric with respect to inversion about the Ti(2) atom.

However, the individual titanium-atom environments are found to be significantly different upon comparing the two Rb/Ti/P/O phases described here and those found in KTP-types. In $Rb_2Ti_3O_2(PO_4)_2(HPO_4)_2$ and $Rb_3Ti_3O(P_2O_7)(PO_4)_3$, the TiO_6 distortions from octahedral regularity, as quantified by the Δ parameter, are as noted above: all the distortions are less than 0.1 Å from geometrical regularity. By comparison, in $RbTiOPO_4$, octahedral distortions, Δ, are 0.426 and 0.344 Å for the two crystallographically distinct titanium atoms, Ti(1) and Ti(2), respectively, indicating substantial displacement of the titanium cation from its geometrical octahedral center, and KTP-types are usually considered to possess a titanyl Ti=O "double" bond [d(Ti–O) < 1.75 Å]. In KTP-type phases, this "polyaromatic" chain of –Ti=O–Ti=O–Ti=O– bonds propagates throughout the crystal.

Several theoretical models have attempted to rationalize the optical response of KTP-type phases on the basis of these short, highly polarizable Ti=O bonds (2, 5). A new theoretical study (33) indicates that the *extended* Ti/O network of distorted TiO_6 groups, as found in $KTiOPO_4$, will tend to have larger hyperpolarizability elements than individual or small numbers of linked TiO_6 groups. However, the presence of other species in KTP isomorphs, notably guest cations such as Na^+ and Ag^+, can have a crucial effect on SHG behavior, as demonstrated for β-$NaTiOPO_4$ and $AgTiOPO_4$ (6), probably via subtle electrostatic polarization effects which alter the band structures in these phases, and consequently attenuate SHG coefficients, even through the geometry of the Ti/P/O frameworks are very similar in all KTP-type materials.

As a closing remark, it should be noted that *all* the bonds in a noncentrosymmetric crystal structure contribute to the overall observed macroscopic SHG coefficient(s) (34). In $Rb_2Ti_3O_2(PO_4)_2(HPO_4)_2$, the asymmetrical PO_3OH groups, and in $Rb_3Ti_3O(P_2O_7)(PO_4)_3$, the P_2O_7 pyrophosphate entity may well make appreciable contributions to the observed SHGs. Thus, a fully-comprehensive analysis of SHG behavior in phases containing TiO_6 groups must take these "secondary" interactions into account. We are continuing our exploratory-synthesis efforts in this area.

ACKNOWLEDGMENTS

We thank Vojislav Srdanov (UCSB) for making the second-harmonic measurements and the National Science Foundation (Division of Materials Research), Grant DMR-9208511, for partial funding.

REFERENCES

1. J. D. Bierlein and H. Vanherzeele, *J. Opt. Soc. Am. B: Opt. Phys.* **6,** 622 (1989), and references therein.
2. G. D. Stucky, M. L. F. Phillips, and T. E. Gier, *Chem. Mater.* **1,** 492 (1989), and references therein.
3. S. J. Crennell, J. J. Owen, C. P. Grey, A. K. Cheetham, J. A. Kaduk, and R. H. Jarman, *J. Mater. Chem.* **1,** 113 (1991).
4. I. Tordjman, R. Masse, and J. C. Guitel, *Z. Kristallogr.* **139,** 103 (1974).
5. B. F. Levine, *Phys. Rev. B* **7,** 2600 (1973).
6. M. L. F. Phillips, W. T. A. Harrison, G. D. Stucky, E. M. McCarron III, J. C. Calabrese, and T. E. Gier, *Chem. Mater.* **4,** 222 (1992).
7. S. J. Crennell, R. E. Morris, A. K. Cheetham, and R. H. Jarman, *Chem. Mater.* **4,** 82 (1992).

8. J. Y. Wang, Y. G. Liu, J. Q. Wei, L. P. Shi, and M. Wang, *Z. Kristallogr.* **191,** 231 (1990).
9. P. A. Thomas, A. M. Glazer, and B. E. Watts, *Acta Crystallogr., Sect. B* **46,** 333 (1990).
10. F. C. Zumsteg, J. D. Bierlein, and T. E. Gier, *J. Appl. Phys.* **47,** 4980 (1976).
11. W. P. Risk, *Appl. Phys. Lett.* **58,** 19 (1991).
12. R. Masse, *Bull. Soc. Fr. Mineral. Cristallogr.* **93,** 500 (1970).
13. S.-M. Wang and S.-J. Hwu, *J. Solid State Chem.* **92,** 219 (1991).
14. P. G. Nagornyi and A. A. Kapshuk, *Russ. J. Inorg. Chem.* **38,** 7 (1993).
15. K. Yvon, W. Jeitscho, and E. Parthe, *J. Appl. Crystallogr.* **10,** 73 (1977).
16. J. P. Dougherty and S. K. Kurtz, *J. Appl. Crystallogr.* **9,** 145 (1976).
17. Data collection and reduction were controlled using a locally modified version of the UCLA Crystallographic Computing Package, developed by C. E. Strouse, Department of Chemistry, UCLA, Los Angeles, CA.
18. G. M. Sheldrick, "SHELXS-86 User Guide." Crystallography Department, University of Göttingen, Germany, 1986.
19. D. J. Watkin, J. R. Carruthers, and P. W. Betteridge, "CRYSTALS User Guide." Chemical Crystallography Laboratory, Oxford University, U.K., 1990.
20. A. C. Larson, *in* "Crystallographic Computing," (F. R. Ahmed, Ed.), p. 291. Munksgaard, Copenhagen, 1970.
21. D. T. Cromer, "International Tables for X-Ray Crystallography," Vol. IV, Table 2.3.1. Kynock Press, Birmingham, 1974.
22. J. R. Carruthers and D. J. Watkin, *Acta Crystallogr., Sect. A* **35,** 698 (1979).
23. P. Main, "MULTAN User Guide." University of York, U.K., 1980.
24. Y. Le Page, *J. Appl. Crystallogr.* **21,** 983 (1988).
25. C. K. Johnson, Oak Ridge National Laboratory Report ORNL-5138, Oak Ridge, Tennessee 37830, 1976, with local modifications.
26. R. X. Fischer, *J. Appl. Crystallogr.* **18,** 258 (1985).
27. R. D. Shannon, *Acta Crystallogr., Sect. A* **32,** 751 (1976).
28. I. D. Brown and K. K. Wu, *Acta Crystallogr., Sect. B* **32,** 1957 (1975).
29. J. A. Kaduk and R. H. Jarman, *Z. Kristallogr.*, **204,** 285 (1993).
30. A. F. Wells. "Structural Inorganic Chemistry," 5th ed., p 859. Oxford, 1986.
31. W. T. A. Harrison, T. E. Gier, G. D. Stucky, and A. J. Schultz, *Chem. Commun.*, 540 (1990).
32. V. K. Yanovskii and V. I. Voronkova, *Izv. Akad. Nauk. SSSR* **25,** 1579 (1989).
33. M. Munowitz, R. H. Jarman, and J. F. Harrison, *Chem. Mater.* **5,** 661 (1993).
34. J. Zyss and J. L. Oudar, *Phys. Rev. A* **26,** 2028 (1982).